

Detailed characterization of a fiber-optic parametric amplifier in phase-sensitive and phase-insensitive operation

Joseph Kakande^{1*}, Carl Lundström², Peter A. Andrekson², Zhi Tong², Magnus Karlsson², Periklis Petropoulos¹, Francesca Parmigiani¹ and David J. Richardson¹

¹Optoelectronics Research Centre, University of Southampton, Southampton, SO17 1BJ, UK

²Photonics Laboratory, Department of Microtechnology and Nanoscience, Chalmers University of Technology, SE-412 96, Gothenburg, Sweden

*jkk@orc.soton.ac.uk

Abstract: We experimentally demonstrate a single-pumped, non-degenerate phase-sensitive parametric amplifier with a precise control of phase and amplitude of the in-going waves and investigate in detail its gain, attenuation and saturation properties in comparison with operation in phase insensitive amplifier (PIA) mode. We experimentally observe the variation of the gain and attenuation as a function of the relative phase, pump power and the signal-idler power ratio. The phase sensitive gain spectrum is studied over a 24 nm symmetrical bandwidth and we achieve a maximum phase sensitive amplification (PSA) gain of 33 dB. A departure from the theoretical maximum attenuation as the gain increases is observed and explained.

©2010 Optical Society of America

OCIS codes: (190.4410) Nonlinear optics, parametric processes; (190.4970) Parametric oscillators and amplifiers; (230.2285) Fiber devices and optical amplifiers; (230.4320) Nonlinear optical devices; (230.4480) Optical amplifiers.

References and links

1. H. A. Haus, and J. A. Mullen, "Quantum Noise in Linear Amplifiers," *Phys. Rev.* **128**(5), 2407–2413 (1962).
2. Y. Mu, and C. M. Savage, "Parametric amplifiers in phase-noise-limited optical communications," *J. Opt. Soc. Am. B* **9**(1), 65–70 (1992).
3. A. Bogris, and D. Syvridis, "RZ-DPSK Signal Regeneration Based on Dual-Pump Phase-Sensitive Amplification in Fibers," *IEEE Photon. Technol. Lett.* **18**(20), 2144–2146 (2006).
4. K. Croussore, I. Kim, Y. Han, C. Kim, G. Li, and S. Radic, "Demonstration of phase-regeneration of DPSK signals based on phase-sensitive amplification," *Opt. Express* **13**(11), 3945–3950 (2005).
5. K. Croussore, and G. F. Li, "Phase regeneration of NRZ-DPSK signals based on symmetric-pump phase-sensitive amplification," *IEEE Photon. Technol. Lett.* **19**(11), 864–866 (2007).
6. K. Croussore, and G. F. Li, "Phase and amplitude regeneration of differential phase-shift keyed signals using phase-sensitive amplification," *IEEE J. Sel. Top. Quantum Electron.* **14**(3), 648–658 (2008).
7. L. Ruo-Ding, P. Kumar, and W. L. Kath, "Dispersion Compensation with Phase-sensitive Optical Amplifiers," *IEEE J. Lightwave Technol.* **12**(3), 541–549 (1994).
8. K. Croussore, and G. Li, "Amplitude regeneration of RZ-DPSK signals based on four-wave mixing in fibre," *Electron. Lett.* **43**(3), 177–178 (2007).
9. M. Sköld, J. Yang, H. Sunnerud, M. Karlsson, S. Oda, and P. A. Andrekson, "Constellation diagram analysis of DPSK signal regeneration in a saturated parametric amplifier," *Opt. Express* **16**(9), 5974–5982 (2008).
10. M. Matsumoto, "Regeneration of RZ-DPSK signals by fiber-based all-optical regenerators," *IEEE Photon. Technol. Lett.* **17**(5), 1055–1057 (2005).
11. M. E. Marhic, C. H. Hsia, and J. M. Jeong, "Optical amplification in a nonlinear fibre interferometer," *Electron. Lett.* **27**(3), 210–211 (1991).
12. W. Imajuku, A. Takada, and Y. Yamabayashi, "In-line Coherent Optical Amplifier with Noise Figure Lower than 3 dB Quantum Limit," *Electron. Lett.* **36**(1), 63–64 (2000).
13. C. McKinstrie, and S. Radic, "Phase-sensitive amplification in a fiber," *Opt. Express* **12**(20), 4973–4979 (2004).
14. O. Lim, V. Grigoryan, M. Shin, and P. Kumar, "Ultra-Low-Noise Inline Fiber-Optic Phase-Sensitive Amplifier for Analog Optical Signals," in *Optical Fiber Communication Conference and Exposition and The National*

- Fiber Optic Engineers Conference, OSA Technical Digest (CD) (Optical Society of America, 2008), paper OML3.
15. R. Tang, J. Lasri, P. S. Devgan, V. Grigoryan, P. Kumar, and M. Vasilyev, "Gain characteristics of a frequency nondegenerate phase-sensitive fiber-optic parametric amplifier with phase self-stabilized input," *Opt. Express* **13**(26), 10483–10493 (2005).
 16. Z. Tong, C. Lundström, A. Bogris, M. Karlsson, P. A. Andrekson, and D. Syvridis, "Measurement of sub-1 dB-Noise Figure in a Non-degenerate Cascaded Phase-sensitive Fibre Parametric Amplifier," in Proceedings of European Conference on Optical Communications, Vienna, Austria 2009, paper 1.1.2.
 17. R. Tang, P. S. Devgan, V. S. Grigoryan, P. Kumar, and M. Vasilyev, "In-line phase-sensitive amplification of multi-channel CW signals based on frequency nondegenerate four-wave-mixing in fiber," *Opt. Express* **16**(12), 9046–9053 (2008).
 18. M. Vasilyev, "Distributed phase-sensitive amplification," *Opt. Express* **13**(19), 7563–7571 (2005).
 19. C. Lundström, J. Kakande, P. A. Andrekson, Z. Tong, M. Karlsson, P. Petropoulos, F. Parmigiani, and D. J. Richardson, "Experimental Comparison of Gain and Saturation Characteristics of a Parametric Amplifier in Phase-sensitive and Phase-insensitive Mode," in Proceedings of European Conference on Optical Communications, Vienna, Austria 2009, paper 1.1.1.
 20. M. Karlsson, "Four-wave mixing in fibers with randomly varying zero-dispersion wavelength," *J. Opt. Soc. Am. B* **15**(8), 2269–2275 (1998).
-

1. Introduction

Phase-sensitive amplifiers have long been known to offer the possibility of amplification with a noise figure (NF) below the 3 dB quantum limit of their PIA counterparts [1]. In addition, considerable interest in them has arisen due to their potential for optical signal processing including parametric phase noise suppression [2] which can be utilised in all optical phase regeneration of phase-encoded signals [3–6] and dispersion compensation [7]. By utilising a PIA in saturation, amplitude regeneration of differential phase shift keying (DPSK) signals has been demonstrated [8,9], and saturated PIAs have also been proposed to reduce accumulated nonlinear phase jitter in transmission links [10]. Saturation of PSAs can provide the added functionality of simultaneous phase and amplitude regeneration [3–6].

PSA in optical fiber systems can be achieved in a nonlinear optical loop mirror [11]. This interferometric loop configuration has been successfully used to demonstrate both sub-3 dB-NF [12] and phase-regeneration of phase-encoded signals [4,6]. However, an interferometric PSA is inherently single-channel, and thus not compatible with wavelength-division-multiplexed (WDM) systems, and the possibility of achieving sub-3 dB-NF is complicated by their susceptibility to guided acoustic wave Brillouin scattering (GAWBS) [12]. PSA can also be implemented in an in-line configuration using four wave mixing in a fibre, avoiding the above two drawbacks of interferometric PSAs. This has been investigated both theoretically [3,13] and experimentally [14]. A non-degenerate FOPA-based PSA requires the injection of three or four waves; one or two pumps, and a signal-idler pair, which then experience amplification or de-amplification. Several different signal-idler pairs can be phase-sensitively amplified at the same time. The interacting waves need to be phase-locked to observe this behavior, and three such phase-locked waves can be derived by using electro-optic modulation (EOM) of a narrow linewidth optical source, producing multiple sidebands locked to the carrier [14]. However, current EOM technology limits the bandwidth achievable via this technique to a few 100 GHz at best. A wideband PSA can be created by cascading two FOPAs, generating a phase-locked but conjugated idler in the first FOPA, and, with a mechanism for changing the relative phase among the waves in between, achieving PSA operation in the second one. This was first demonstrated in [15], using a short dispersive fiber to introduce a wavelength-dependent phase shift through dispersion. The same method was used in [16] to demonstrate a sub-quantum limit NF of the PSA stage. However, it should be noted that the NF of the combined system will be limited by the 3 dB quantum limit of the PIA stage. In addition, this cascaded system cannot be directly employed for phase regeneration due to the absence of an absolute phase reference synchronized to both the signal and pump. In the presence of such a phase locking system, phase regeneration can only

be achieved if the signal and idler at the PSA input are coherent copies of each other, and not phase conjugates as in the cascaded PSA setup [17].

From simple theory [18] the maximum/minimum phase sensitive gain can be expressed as $G_{\max/\min} = [G_{\text{PIA}}^{1/2} \pm (G_{\text{PIA}} - 1)^{1/2}]^2 = \exp(\pm 2gz)$, where G_{PIA} is the phase insensitive gain, g is the parametric gain coefficient and z is the fiber length. Thus, the parametric attenuation of the quadrature phase component should be the inverse of the gain of the in-phase component. In addition, the maximal phase sensitive gain should be four times larger than the phase insensitive gain. A PSA with an attenuation that is not the inverse of the gain will have an impaired noise figure and phase-regeneration performance. In this paper, we present the detailed characterization results of the PSA's and PIA's behavior, including corresponding gain, attenuation and saturation performances, which were preliminarily reported in [19]. We also discuss possible causes of the observed compromised phase dependent attenuation and show measurements of the PSA as a black box device in which signal gain can be altered by varying the power of the internal pump and idler waves.

2. Experimental setup

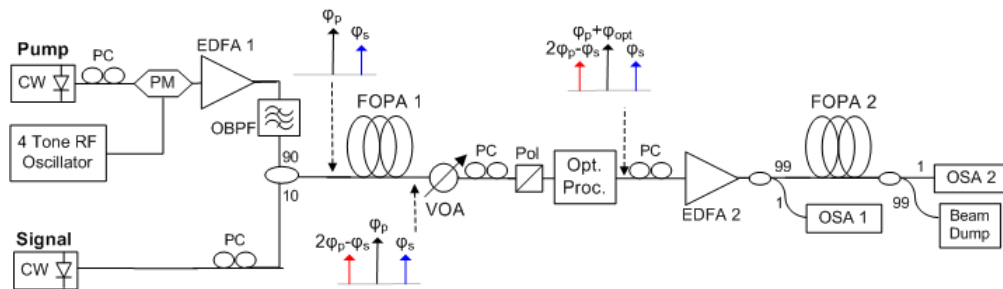


Fig. 1. Phase sensitive amplifier setup based on cascaded FOPAs with precise phase and amplitude tuning between the two stages together with the sketch of the phases of the various waves as they propagate through the system. PM: phase modulator, EDFA: erbium doped fibre amplifier, PC: polarization controller.

The experimental setup is shown in Fig. 1. A tunable laser (TL) set at 1553.0 nm was used as a pump source. Unless stated otherwise the pump was phase modulated with four RF tones at approximately 100, 300, 900 and 2700 MHz, increasing the pump linewidth up to 10 GHz to suppress Stimulated Brillouin Scattering (SBS). The pump was then amplified to 3.8 W by EDFA1, and filtered by a 2 nm-bandwidth optical bandpass filter (OBPF) to suppress generated amplifier spontaneous emission (ASE). A second tunable laser was used as the signal source and the pump and signal were coupled via a 10 dB coupler into FOPA1, see Fig. 1, where a conjugated idler is generated by the four wave mixing process. FOPA1 was implemented using a 150 m long highly nonlinear fiber (HNLF), with a nonlinearity coefficient of $10 \text{ (W}\cdot\text{km)}^{-1}$ and zero-dispersion wavelength (ZDW) of 1542 nm. The output, consisting of three phase locked waves, was then passed through a 10 dB coupler, a polarizer and a variable optical attenuator (VOA). The polarizer provided a polarization reference for all three waves going into FOPA2 and ensured that the signals were aligned with the principal axis of EDFA2 in order to minimize the differential group delay (DGD) in EDFA2. After the polarizer, the waves were subsequently passed through an optical processor (Opt. Proc., Finisar Waveshaper 4000E) by which the desired relative amplitudes and phases could be set. The processor also allowed for very narrow filtering of the pump wave, removing any residual ASE. The three waves were then amplified by EDFA2 up to 2 W, with the pump signal completely dominating the power, and injected into FOPA2. FOPA2 was implemented with a 250 m HNLF with nonlinearity coefficient of $11.7 \text{ (W}\cdot\text{km)}^{-1}$ and a ZDW of 1542 nm.

The input into and output from FOPA2 were monitored on two optical spectrum analyzers (OSAs) via two 20 dB couplers.

The PSA gain or attenuation is governed by the total relative phase, φ_{rel} , among the three interacting waves. It is defined as $\varphi_{rel} = 2\varphi_p - \varphi_s - \varphi_i$, with φ_p , φ_s and φ_i being the absolute phases of the pump, signal and idler waves, respectively. φ_{rel} is constant after FOPA1, regardless of the changes in phase of the input waves, since FOPA1 is phase-insensitive. Note, however, that any wavelength dependent effects, such as dispersion, between FOPA1 and FOPA2, will change the φ_{rel} value at the input of FOPA2. By changing the phase of one or more of the waves with the optical processor, φ_{rel} at the input of FOPA2 can be set to an arbitrary value. Figure 1 shows a schematic illustration of the phases of the various waves as they propagate through the system components. In the experiment we chose to change φ_{rel} , adding φ_{opt} to the pump phase, i.e. $\varphi_{p'} = \varphi_p + \varphi_{opt}$, where $\varphi_{p'}$ is the pump phase after the optical processor. The idler wave can also be blocked entirely in the optical processor, changing the FOPA2 operation from PSA to PIA. In addition, the various channels in a typical wideband PSA exhibit peak phase sensitive gains at differing input relative phases due to the impact of dispersion in the PSA HNLF [17]. A device such as the optical processor which provides precise phase tuning of selectable spectral windows over a wide bandwidth enables multi-channel PSA applications which is required in addition to the phase locking of signal, idler and pump waves.

3. Results

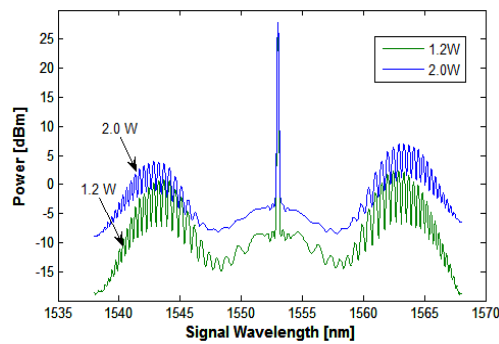


Fig. 2. FOPA2 output spectra when pump and ASE from FOPA1 are coupled into FOPA2 without mid-stage filtering.

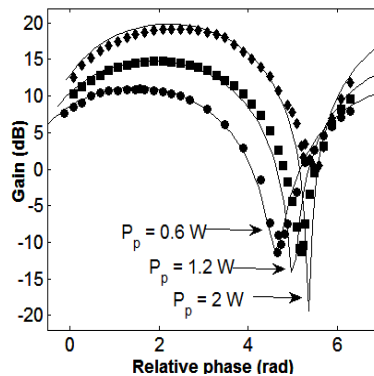


Fig. 3. PSA phase dependent gain at varying pump powers with signal and idler powers equalized. Lines are theoretical curves.

With the signal laser off and the optical processor configured so as to couple the parametrically amplified ASE from FOPA1 into FOPA2, it is possible to quickly characterize the system in terms of bandwidth, peak gain, and with limited accuracy, phase sensitivity. Figure 2 shows output spectra from FOPA2 using pump power levels of 1.2 W and 2 W in FOPA2, while keeping constant the pump power in FOPA1. The symmetric gain peaks can be seen around 1563 and 1543 nm, with the bandwidth being slightly more with the stronger pump. Because the input ASE signal was attenuated by 10dB between the two stages in the 2W pump case in order to suppress saturation in FOPA2 the absolute increase in the peak gain from 1.2 to 2 W pumping for FOPA2 cannot be determined from Fig. 2 alone. The ripple in the curves is a clear sign of PSA, with dispersion between the two FOPAs causing a wavelength dependent relative phase modulation [15]. As the dispersion-induced phase scales quadratically with wavelength, the rippling effect becomes greater as detuning from the pump increases. It is also worth noticing that, contrary to expectations, the difference between maximum and minimum gain is reduced in the case of higher pump power. An explanation for this behaviour will be discussed below.

Figure 3 shows the variation of gain as a function of the relative phase for a signal at 1 nm detuning from the pump at three different pump power levels, 0.6, 1.2 and 2 W respectively. The signal and idler powers were equalized and kept 30 dB lower than the pump. Care was taken to ensure that any slow gain or polarization drifts in FOPA1 which propagate through to FOPA2 were periodically compensated for by adjusting the optical processor's setting. At lower pump power, and consequently lower gain (circles), the maximal amplification is the same as the maximal attenuation (11 dB at 0.6 W pump power). However, as the pump power increases, this behavior is lost. The theory [18] predicts that the PSA gain varies sinusoidally with the relative phase as can be seen in Fig. 3. However, on a logarithmic (dB-) scale, the parametric attenuation peak (or gain "dip") will be significantly narrower than the gain peak, and far more so for high PSA gain/attenuations. Consequently, more stringent phase control is required to observe the increased maximal attenuation at higher gains and there is reduced tolerance to phase disturbances introduced by noise or wavelength jitter.

To study the sensitivity of the PSA to the signal and idler power ratio, the idler was systematically attenuated compared to the signal and the signal phase dependent gain recorded, as shown in Fig. 4. As expected, as the signal becomes significantly greater than the idler, the maximal gain and attenuation decrease and approach the gain of the PIA. Furthermore, the maximal attenuation drops off much faster than the maximal gain. It is worth noting that in Fig. 4, a signal/idler relative fluctuation of 1dB from the 0 dB optimal point would lead to a fluctuation in the phase dependent extinction of 7.5 dB, of which 7 dB would be due to reduced PSA attenuation, and only 0.5 dB due to reduced maximal PSA gain. Such a fluctuation would have an impact on the device noise figure due to the reduction in squeezing achieved.

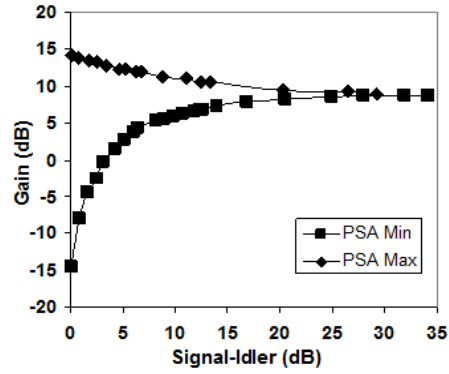


Fig. 4. PSA gain as the signal-to-idler power ratio is varied. The lines are respective results of simulations using the same parameters as in the experiment. Pump power is 1.2W and two modulation tones were used.

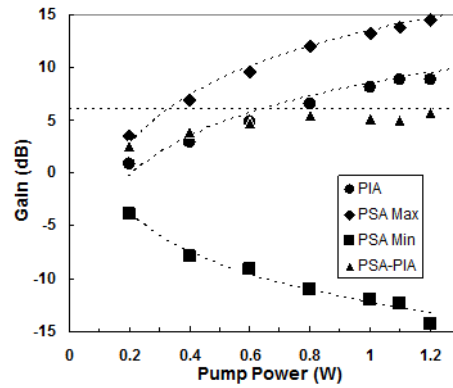


Fig. 5. Measured PIA (circles), PSA maximum (diamonds), PSA minimum (squares) and difference between PIA and PSA maximum (triangles) gains of FOPA2 versus pump power. Two modulation tones were used.

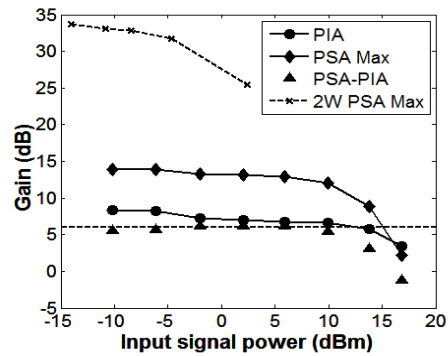


Fig. 6. Measured PIA (circles), PSA maximum (diamonds) and difference between PIA and PSA maximum (triangles) gains of FOPA2 versus input signal power at 1nm detuning and 1.2W pump. Dashed line shows PSA gain at the gain peak with 2W pump

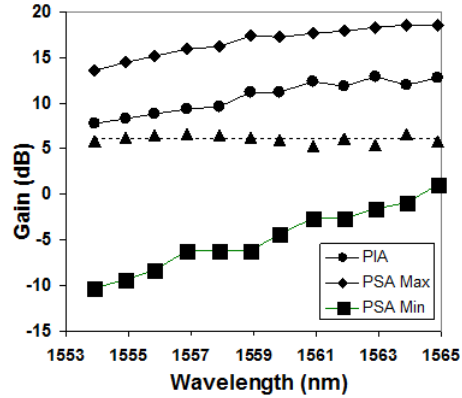


Fig. 7. Measured PIA gain (circles), PSA maximum gain (diamonds), PSA maximum attenuation (squares) and difference between PIA and PSA gain (triangles) gains of FOPA2 as a function of the signal wavelength with pump power of 1.2 W.

The pump power was varied and the phase dependent gain recorded as shown in Fig. 5 for a signal at a 1 nm detuning from the pump. As the pump power increases, the maximum phase sensitive gain increases by approximately 1.5 dB/dB, and the maximum phase sensitive attenuation by -1.2 dB/dB. The difficulty in achieving the theoretical maximal attenuation demonstrates the limited maximal attenuation demonstrable with this experimental technique. The difference between the maximal phase sensitive and the phase insensitive gain is also seen to approach 6dB beyond a pump power of 0.8W. Furthermore, the maximum difference (extinction) between the phase sensitive gain and attenuation we achieved was 30dB. While a higher figure of 35 dB has been previously demonstrated [5] using a Bismuth oxide fibre, the real fibre gain was not stated. However, we believe that the use of germanium doped HNLf in this instance with significantly lower losses should allow higher peak gains.

An investigation of the gain saturation properties of the PSA was carried out by increasing the signal/idler power, while keeping the input pump power constant at 1.2 W (still at 1 nm detuning from pump). The resulting FOPA2 gain is shown in Fig. 6, with a measured PSA dynamic range of about 23 dB. Since the maximum gain achievable for the PSA case is higher, it saturates before the PIA gain as can be seen by the reduction in the PSA-PIA gain difference (triangles in Fig. 6) from the theoretical maximum of 6 dB. Additional measurements revealed no saturation for the minimum phase sensitive gain as would be expected. By moving the signal wavelength to 1563.8 nm, which corresponds to the PSA gain peak, and increasing the pump power to 2 W, we were able to achieve 33 dB of PSA gain. Because the ASE noise from EDFA2 at that pump power imposed relatively high minimum powers for the input signal/idler, we could not achieve unsaturated gain. The difference between PSA and PIA gain was therefore less than 6 dB. Nevertheless, PSA behavior was confirmed by changing the FOPA2 input relative phases and observing the output signal power variations.

Figure 7 shows the measured characteristics of the PIA gain, maximum PSA gain and maximal PSA attenuation of FOPA2 as the signal and idler wavelengths were detuned from the pump. The maximum PSA gain increases with detuning up to 19 dB at the gain peak for a pump power of approximately 1.2 W. The gain extinction is highest closest to the pump, and reduces steadily towards the PSA gain peak. This is due to a combination of phenomena. Firstly, as discussed earlier, as the maximal gain increases the tolerance required to achieve maximal attenuation becomes stricter. Secondly, the use of pump dithering to suppress SBS meant that the pump and idler had linewidths on the order of 10 GHz. This rapid variation in wavelength is translated to a rapid variation in phase through dispersion, and thereby distorts the relative phase. The tolerance to relative phase variations is lower closer to the gain peak

(this can also be noted in the ripples in Fig. 2, which increase as the signal wavelength detuning increases). In addition, the polarization mode dispersion (PMD) in EDFA2, which was estimated to be around 0.5 ps will certainly have meant that the polarization states of the various waves relative to each other at the input to FOPA2 will have varied as the detuning was increased, leading to compromised phase dependent gain. Also, as the spacing in wavelength from the pump increases, longitudinal ZDW fluctuations act to randomly detune the relative phase between the propagating waves from that precise value required for maximal attenuation [20].

4. Conclusions

We have demonstrated a non-degenerate PSA that allows for precise control of the ingoing signal and idler powers, as well as the relative phase. We carried out a detailed study of the PSA gain and attenuation statically by varying the relative phase, signal/idler wavelength, pump power and signal/idler absolute power and power ratio. We measured a phase-sensitive gain of 33 dB, which we believe is the highest reported to date, and a PSA symmetrical operation bandwidth of 24 nm. We also investigated the saturation properties of the PSA, finding that the PSA saturates at lower input signal powers than the PIA, but the maximal attenuation remains unaffected, in accordance with theory. We also noted the large sensitivity of the parametric attenuation to fluctuations in both phase and power. A practical PSA requires this strict power and phase control dynamically, and emphasizes the need for the development of very high-performance phase-locking solutions, passive SBS suppression techniques so as not to broaden the pump linewidth, as well as the possible need for polarisation maintaining components for future PSA implementations. Achieving a large phase-sensitive attenuation is fundamentally more difficult than a large phase-sensitive gain, but is crucial in order to achieve both good phase regeneration and a noise figure approaching 0 dB, two of the most intriguing promises of phase-sensitive amplifiers.

Acknowledgments

The research leading to these results has received funding under the European Communities Seventh Framework Programme FP/2007-2013 under grant agreement 224547 (PHASORS).